# Release of Gas-Phase Halogens by Photolytic Generation of OH in Frozen Halide−Nitrate Solutions: An Active Halogen Formation Mechanism?

**J. Abbatt,*,† N. Oldridge,† A. Symington,‡ V. Chukalovskiy,† R.D. McWhinney,† S. Sjostedt,† and R.A. Cox‡**

*Department of Chemistry, University of Toronto, 80 St. George St., Toronto, ON, M5S 3H6, and Department of Chemistry, University of Cambridge, Lensfield Road, Cambridge, U.K., CB2 1EW*

*Received: March 8, 2010; Revised Manuscript Received: May 5, 2010*

To better define the mechanisms by which condensed-phase halides may be oxidized to form gas-phase halogens under polar conditions, experiments have been conducted whereby frozen solutions containing chloride (1 M), bromide ($1.6 \times 10^{-3}$ to $5 \times 10^{-2}$ M), iodide ($<1 \times 10^{-5}$ M), and nitrate (0.01 to 1 M) have been illuminated by ultraviolet light in a continually flushed cell. Gas-phase products are quantified using chemical ionization mass spectrometry, and experiments were conducted at both 248 and 263 K. $Br_2$ was the dominant product, along with smaller yields of IBr and trace BrCl and $I_2$. The $Br_2$ yields were largely independent of the $Br^-/Cl^-$ ratio of the frozen solution, down to seawater composition. However, the yields of halogens were strongly dependent on the levels of $NO_3^-$ and acidity in solution, consistent with a mechanism whereby $NO_3^-$ photolysis yields OH that oxidizes the condensed-phase halides. In support, we observed the formation of gas-phase $NO_2$, formed simultaneously with OH. Gas-phase HONO was also observed, suggesting that halide oxidation by HONO in the condensed phase may also occur to some degree. By measuring the production rate of condensed-phase OH, using benzoic acid as a radical trap, we determine that the molar yield of $Br_2$ formation relative to OH generation is 0.6, consistent with each OH being involved in halide oxidation. These studies suggest that gas-phase halogen formation should occur simultaneously with $NO_x$ release from frozen sea ice and snow surfaces that contain sufficient halides and deposited nitrate.

## 1. Introduction

It is now well recognized that the snowpack is a chemically complex environment, consisting of a wide range of organic species, either formed biogenically or deposited from the atmosphere, and inorganic species, such as deposited nitrate and halides. So, the discoveries that have been made of late that indicate that this environment can be highly chemically active are not too surprising.[1] In particular, it is now known that the snowpack can also act as a source of small volatile organic compounds (VOCs) to the atmosphere,[2] especially with the increased illumination and higher temperatures associated with daytime, and that photolytic $NO_x$ release occurs in the form of both $NO_2$ and HONO.[3,4]

The goal of this work is to examine whether the snowpack also has the potential to be a source of gas-phase active halogens, through photolytic processes. Given known chemistry, it is likely that halide oxidation will occur in ice environments where both nitrate and halides are present. In particular, photolysis of nitrate is a source of condensed phase OH radicals, through reaction 1, where the $O^-$ species that is formed will readily abstract a proton from either water or an acid:[5]

$$NO_3^- + h\nu \rightarrow NO_2 + O^- \quad (1)$$

$$NO_3^- + h\nu \rightarrow NO_2^- + O \quad (2)$$

The branching ratio between reactions 1 and 2 favors the former channel, by which OH is generated.[6,7] Anastasio and co-workers have confirmed that in frozen solution substrates, OH is indeed formed in a manner similar to that which prevails in water.[7] Also, $NO_2$ and HONO have been observed from these photoreactions occurring in ice.[8,9] The HONO may form either from protonation of $NO_2^-$ or by secondary chemistry arising from $NO_2$.[10]

Once OH is generated, it will react with chemically reduced species, such as halides and organics. In the case of halides, it was shown many decades ago that the ultimate fate of photolytically generated OH radicals in seawater is to preferentially oxidize $Br^-$ over $Cl^-$, even though the concentration of $Br^-$ is close to three orders magnitude lower than that of $Cl^-$.[11−13] Frinak and Abbatt confirmed that $Br_2$ is indeed released from seawater solutions when exposed to gas-phase OH radicals that interact heterogeneously with the solution substrates.[14] These results were in line with those of Oum et al. who inferred that $Cl_2$ is formed when OH interacts with aqueous particles containing NaCl.[15] Finally, George and Anastasio demonstrated that a gas-phase species containing bromine was formed when nitrate photolysis proceeds in a bromide-containing aqueous solution.[16]

Putting these findings together, it is reasonable to hypothesize that $Br_2$ production will proceed if nitrate photolysis occurs in frozen aqueous media. However, experimental confirmation is necessary to show the mechanism is viable. For example, can OH oxidation of halides occur sufficiently fast to give high halogen yields, compared to potential radical−radical recom-

* To whom correspondence should be addressed.
† University of Toronto.
‡ University of Cambridge.

10.1021/jp102072t 
Published on Web 05/19/2010

bination steps, such as the reverse of reaction 1 or the reaction of OH with $NO_2$? Are the halogens released from the ice substrates efficiently, or are they subject to chemical loss, perhaps via reaction with condensed-phase OH? Which halogens are formed, and at what relative rates? Our first attempt to address these general issues was presented in a paper where we demonstrated the gas-phase production of halogens, principally $Br_2$ with smaller yields of BrCl and IBr, when gas-phase OH radicals are exposed to frozen halide solutions and humidified salts.[17] However, to our knowledge, this is the first attempt to demonstrate that halogen production proceeds photolytically, from frozen halide solutions that contain an OH precursor. We also consider the possibility that halogen production may proceed via formation of HONO, generated in Reaction 2. In particular, HONO is known to oxidize bromide in acidic ice substrates, giving rise to BrNO formation (although $Br_2$ formation has not yet been observed as a product).[18,19]

Although now widely recognized, the overall motivation for understanding the formation of active halogens, both bromine containing but also chlorine and iodine as well, is that high levels of bromine have been observed to be associated with depletion of ozone and mercury at polar latitudes in the springtime.[20,21] The mechanisms for loss of such species under an environment of high gas-phase active bromine loading are relatively well understood, but the source of the bromine remains unquantified two decades after the initial ozone depletion events were observed. In particular, a "bromine explosion" driven by the autocatalytic release of $Br_2$ after HOBr uptake by the snowpack is likely important at high active bromine levels,[22] but the bromine activation process at low bromine loadings and the process that drives initial bromine release remain poorly quantified. Without knowledge of the most important bromine release initiation mechanism(s), our models do not yet have predictive abilities for these ozone and mercury depletion events.

So, to better understand the formation of halogens under polar conditions, the experiments described below were designed with three specific goals in mind. First, are gas-phase halogens formed from frozen solutions containing halides and an OH photolytic precursor? Second, how does the production rate of these halogens vary with experimental parameters such as temperature, halide concentration, nitrate concentration, and acidity? What chemical mechanism is consistent with these findings? And, finally, what is the yield of halogens relative to the OH production rate? That is, what fraction of OH radicals formed go on to oxidize halides? If halogens are formed in stoichiometric amounts exceeding the production rate of OH, does this imply a role for HONO as an oxidant?

## 2. Experimental Section

The reaction cell has been described previously[9] and is illustrated in Figure 1. It is a cylindrical glass vessel, 8 cm high with a radius of 5 cm. It is surrounded by another glass vessel, similar in shape but larger, through which coolant flows. There are three openings in the reaction cell: a transparent, fused-silica cover to allow for the addition of sample and ultraviolet light, an inlet for gas to be flowed in, and an outlet to allow gases to escape. These two openings allow gaseous nitrogen to pass through the cell, from the bottom to the top, carrying with it any gases that may evolve from the ice.

There are three on/off valves to control the flow of nitrogen in and around the cell. When valve 2 (Figure 1) is open and valves 1 + 3 are closed, nitrogen bypasses the reaction cell entirely. This is referred to as bypass mode. In the opposite scenario, 1 + 3 are open and 2 is closed, and nitrogen is routed

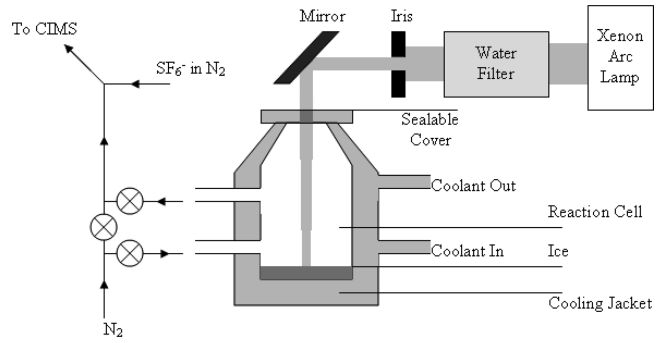


**Figure 1.** Photolysis Cell. Products that enter the gas phase are swept away to the CIMS when valves 1 + 3 are open.

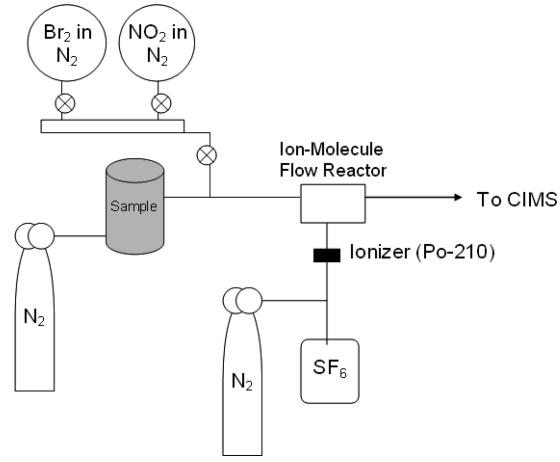


**Figure 2.** Simplified schematic of the overall experimental apparatus.

through the cell, that is, reaction mode. Each run starts in bypass mode while the ice sample is being prepared, and the pressure in the reaction cell is the same as the ambient pressure. Once the cell is opened in reaction mode, the pressure inside the reaction cell decreases to the operating conditions of the experiment, 90 Torr.

Light from a 1000 W xenon arc lamp was passed through a water filter to remove infrared, through an iris to control beam width, and then reflected off a concave spherical mirror before being focused onto the ice surface. Any photochemical reactions would occur in the ice at or below the surface where light shone, which covered a circular area approximately 1.5 cm wide. We assume the area of ice illuminated is approximately 2 $cm^2$. The spectrum of such lamps is not dissimilar to that of the sun, but it does extend to below 300 nm, the threshold for ground level actinic radiation. However, we used an unfiltered lamp for these experiments to maximize the photolysis rate of nitrate, which absorbs strongly below 300 nm as well. Because nitrate photolysis only acts as the OH source for this work, we feel that using UV below 300 nm does not affect the environmental relevance of the results that are presented.

The overall experimental apparatus is shown in Figure 2. The outflow of nitrogen gas (190 sccm) containing the products is sent to an ion−molecule reaction flow tube of a chemical ionization mass spectrometer (CIMS), where the products mix with an ionized gas. A dilute mixture of $SF_6$ in $N_2$ (8.0 L/min) is sent through a Po-210 static charge eliminator (NRD LLC, Grand Island, NY, USA). Here, $SF_6$ is ionized by electron attachment to $SF_6^-$. $SF_6^-$ was chosen as the ionizing reagent within the ion−molecule flow tube because of its ability to ionize many different gases, including $NO_2$, $Br_2$, and other

halogens.[23] The interaction between $SF_6^-$ and gases in the ion−molecule flow tube generates product ions that pass to the ion optics region of a mass spectrometer system. A single linear quadrupole is set to selectively pass particular ions, which are detected with a Channeltron electron multiplier. The mass spectrometer has been described previously.[24]

Glass bulbs of trace $Br_2$ (from liquid $Br_2$, min 99.5%, ACP chemicals) in $N_2$ and $NO_2$ (from liquid $N_2O_4$, Specialty Gases of America, Toledo, OH) in $N_2$ were prepared in known mixing ratios. They were used for quantitative calibration of the CIMS by addition of known flows under the operating conditions of the experiment.

Solutions were prepared by dissolving NaCl (ACP Chemicals, 99.0%), NaBr (Sigma-Aldrich, 99.0%), and $NaNO_3$ (Fisher Scientific, 99.2%) in filtered water (resistance >18 MΩ). The NaCl concentration was 1.0 M for most experiments, NaBr concentration varied from 1.6 to 50 mM, and $NaNO_3$ varied in concentration from 10 mM to 1 M. The NaCl contained an iodide impurity, $< 1 \times 10^{-5}$ M NaI. Acidity of the solutions was controlled by addition of dilute sulfuric acid (diluted from 96% assay, Fisher Scientific).

With the reaction cell in bypass mode, 7 mL of solution were added to the cell. Solutions at 263 K would remain liquid until the cell was changed to reaction mode. At this point, the pressure inside the cell would decrease from ambient pressure to 90 Torr, and evaporative cooling caused the solution to freeze from top to bottom over a time of 1−3 s.

Signals from the CIMS were allowed to stabilize, at which time the photolysis lamp was turned on. The mirror and cell position were adjusted manually until the illuminated spot on the ice was as bright as possible and about 2 $cm^2$ in area. This is the area used in calculations of gas-phase product flux. After the product signals had remained stable for some time, the lamp was turned off and the evolution of the product signals was monitored for a short time.

Up to 10 different masses were monitored, for 0.5 s each. Thus, each ion was measured at a time resolution of no more than 5 s. However, typically, fewer species were monitored because of lack of signal at all mass-to-charge ratios. Ions were monitored at $m/z = 146$ ($SF_6^-$), 124 ($SF_4O^-$, from reaction with $H_2O$), 46 ($NO_2^-$, from reaction with $NO_2$), 62 ($NO_3^-$, probably from reaction with $HNO_3$), 160 ($Br_2^-$ from reaction with $Br_2$), 206 ($IBr^-$ from reaction with IBr), 254 ($I_2^-$ from reaction with $I_2$), 116 ($BrCl^-$ from reaction with BrCl), and 70 ($Cl_2^-$ from reaction with $Cl_2$). We also monitored $m/z$ 66, which we attribute to $FHNO_2^-$. This ion is known to arise from $SF_6^-$ reacting with HONO. However, there is also the potential for HF, formed by $SF_6^-$ reacting with $H_2O$, to react with $NO_2^-$ to form this cluster.

Calibrations were performed by metering a constant flux of $Br_2$ or $NO_2$ from the gas manifold, of fixed volume and temperature, connected to the $Br_2$ and $NO_2$ reservoirs. The pressure drop per unit time from the manifold was converted to the number of $Br_2$ or $NO_2$ molecules released per unit time. This gas release generated a CIMS signal in counts per second (cps) on top of the background signal, so we could determine a sensitivity in units of cps per molecule/s. In all cases, we normalized the observed signals and sensitivities to the $SF_6^-$ reagent ion signal prevalent during the experiment. For each experiment, the signal intensities that were stable with time were averaged to calculate the signal generated while the lamp was on. Using the calibrated sensitivity, we could then determine the flux of molecules per second that evolved from the ice. Dividing by the area that is illuminated (approximately 2 $cm^2$) gives the rate of halogen evolution from the ice, in units of molecules/$cm^2$/s. Note that by expressing the fluxes per unit surface area we do not mean to imply that heterogeneous chemistry is driving the release; it is simply a convenient manner by which to express the results.

These calibrations allowed us to determine our detection limits, calculated for $S/N = 1$ where the noise is the standard deviation of our background signal, that is, this is the amount of signal that we assume we can distinguish from background noise. Depending on the operating conditions (such as the age of the radioactive source), our detection limit for $NO_2$ varied from $2 \times 10^{11}$ to $2 \times 10^{12}$ molecules/s, and for $Br_2$, from $7 \times 10^9$ to $8 \times 10^{10}$ molecules/s.

Calibrations were not performed for BrCl, IBr, and $I_2$. We assume that the CIMS is equally sensitive to each of these as it is to $Br_2$, given that their gas-phase electron affinities are so similar to each other and to $Br_2$.[25] That is, we are assuming that each of these dihalogens has the same collision-controlled ion−molecule rate constant with $SF_6^-$ as $Br_2$. Calibrations of HONO were not performed, and so we do not report flux data for this photoproduct. In addition, as described above, we are not fully confident that mass spectral intensity at $m/z$ 66 is all due to HONO.

We believe that the variability of the results, which is typically a factor of 2 but occasionally higher, is larger than systematic uncertainties arising from the calibrations (which are on the order of ±20% or so). The experimental variability was hard to pin down specifically, but we believe it is probably due the nature of the freezing process and the associated effects on the flux of light in the ice matrix, for example, via multiple scattering. It may additionally be due to the variability associated with aligning the light source into the cell for each experiment and the variations in the lamp output during the few month duration of the experiments.

For the quantification of hydroxyl radical generation, we used the benzoic acid radical trap method as described by Chu and Anastasio.[7] Sodium benzoate (>99.5%, Fluka) is added to the reaction vessel at a concentration of 10 mM. Using a simple kinetics model of the aqueous phase experimental conditions,[14] it can be shown that at this concentration OH will react quantitatively with benzoic acid, producing *p*-hydroxybenzoic acid. The yield is 0.063 ± 0.014.[7] The *p*-hydroxybenzoic acid product was quantified with an HPLC fitted with a 100 μL injection loop, a CSC-inertsil 150A C-18 column (10 × 0.46 cm, 5 μm packing), and a UV-absorbance detector, monitoring at 256 nm. The separation was accomplished by three-step gradient elution at 1 mL/min flow rate during the first step and 1.8 mL/min flow during the second and the third steps. The mobile phase consisted of 13% acetonitrile and 87% of water acidified with 0.13% trifluoroacetic acid during the first 3.5 min step. The mobile phase contained 35% ACN and 65% acidified water during the second 3 min step. The mobile phase was changed back to 13% ACN and 87% acidified water during the third 5 min step. The gradient elution method gave clearly resolved peaks of benzoic, *p*-hydroxybenzoic, and *m*-hydroxybenzoic acids. Calibrations of *p*-hydroxybenzoic acid (>99%, Fluka) were performed daily.

## 3. Results and Discussion

**3.1. Initial Observations.** Typical results are shown in Figure 3 for selected ions. In particular, significant production of IBr, $Br_2$, $NO_2$, and potentially HONO is observed. There is a small change in the reagent ion signal with the products being formed, but we account for this, as mentioned above, by referencing all signals to the intensity of the reagent ion, when fluxes were

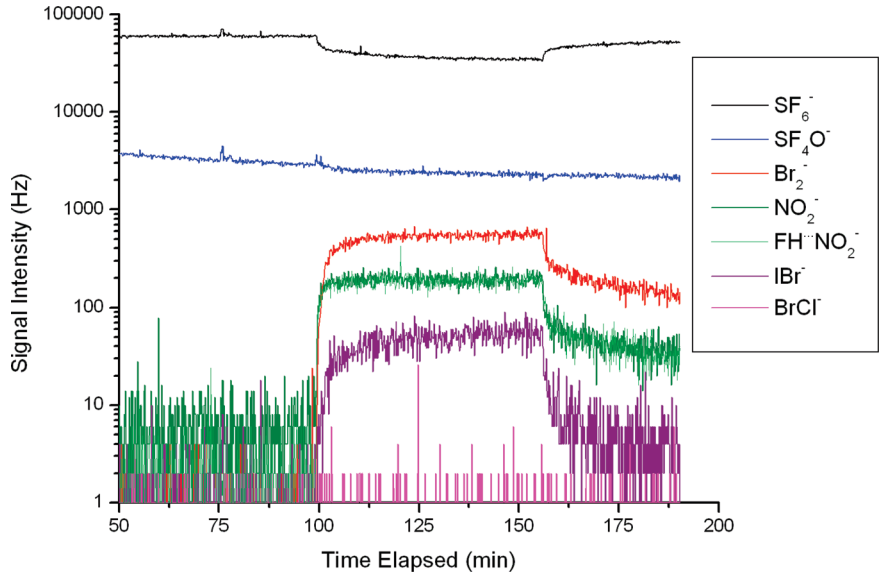


**Figure 3.** Typical output from a photolysis experiment. The system is allowed to equilibrate until 100 min, at which point the lamp is turned on. Signal intensities of $Br_2$, $NO_2$, IBr, and probably HONO all increase upon illumination, suggesting that they are products or byproduct of nitrate photolysis. This output is from a frozen solution of 1 M NaCl, 1 M $NaNO_3$, 0.05 M NaBr, pH 2.5, at 248 K.

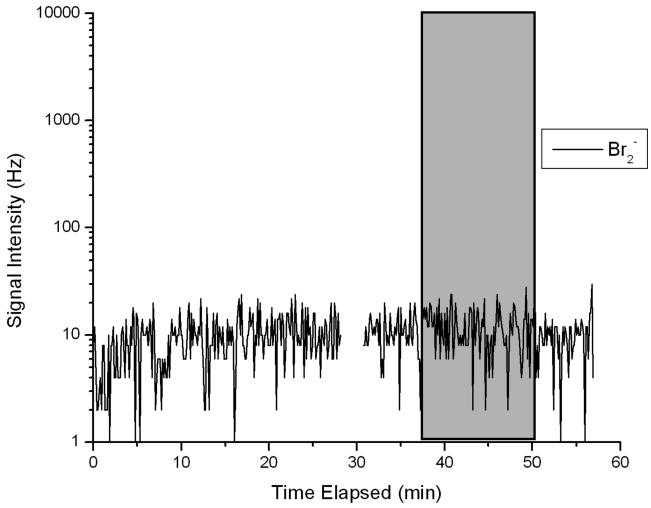


**Figure 4.** $Br_2$ signal from a frozen solution of 1.0 M NaCl, 0.05 M NaBr, pH = 2.5. The highlighted time, from 37 to 51 min, indicates when the lamp was on.

calculated. By contrast, no $Br_2$ was seen to evolve from solutions that did not contain nitrate (Figure 4). Note that there were small and variable backgrounds at some mass-to-charge ratios, notably those for $Br_2$, probably arising from the stickiness of this molecule on the surfaces of sampling lines.

It is also worth noting that while $Br_2$ and IBr are the dominant halogen products, $I_2$ and BrCl were also detected in some experiments, albeit at levels close to our detection limit. Fluxes of all species from the ice are documented in Table 1.

In Figure 3, it is seen that after the lamp was turned off, each product ion signal decreased rapidly but not to background. We interpret this behavior as due to slow diffusion of photoproducts from the ice/brine mixture. The time scale for the release of these trapped products is more consistent with diffusion from an aqueous substrate than from a pure ice matrix, with very low diffusion coefficients.

Our observation of $NO_2$ production is qualitatively corroborated by previously published laboratory studies showing that illuminated frozen nitrate solutions produce $NO_2$.[8,9]

**3.2. Effect of Nitrate Concentration on $Br_2$ Production.** To help evaluate the mechanism for the halogen release, solutions of 1 M NaCl, 0.05 M NaBr, and pH 2.5 were prepared with varying amounts of nitrate. At 248 K, solutions containing more nitrate produced more $Br_2$ (Figure 5), with the effect saturating at high nitrate concentrations. In early experiments at 263 K (data not shown), the same general trend of saturation was also apparent.

The saturation effect in the $Br_2$ production rate with increasing nitrate concentrations is understood from the optical thickness of the solutions in the ultraviolet. For the most concentrated solutions (i.e., 1.0 M), essentially all the light (for example, between 280 and 300 nm) is absorbed within the 0.4 cm depth of the frozen ice substrate, as calculated using the Beer−Lambert Law and the absorption coefficients from Chu and Anastasio.[7] Thus, increasing the concentration of nitrate further will not lead to additional photolysis in solution. However, for concentrations of 0.1 M and lower, the light attenuation is approximately linear as a function of depth, that is, not all the light is getting absorbed. In the nonsaturated regime, the increasing fluxes of $Br_2$ will be arising through increased rates of nitrate photolysis, and so also OH production. We note that the shape of the bromine production curve as a function of nitrate concentration resembles the analogous curve for the aqueous reaction.[16]

**3.3. Effect of Bromide Concentration on $Br_2$ Production.** With other variables held constant, varying the concentration of bromide by over a factor of 30 in the ice did not affect $Br_2$ fluxes (Figure 6), within the limit of our uncertainties. Note that the lowest concentration in Figure 6 is 1.6 mM, just twice the level of bromide present in seawater. This observation is consistent with efficient scavenging of photolytically generated OH by bromide, that is, as demonstrated for seawater by Zafiriou[13] and by George and Anastasio.[16] In our case, where freezing will be concentrating the halide salts into brine pockets or films, it is even more likely that the levels of bromide will be sufficiently high that it becomes the prime scavenger for the OH radical.

**3.4. Effect of Temperature on Halogen Release.** $Br_2$ and $NO_x$ production both show a clear temperature dependence. For otherwise identical conditions, solutions frozen to 263 K

**TABLE 1: Experimental Data**

| | | | | | | fluxes, molecules/cm$^2$/s/10$^{11}$ | | | | |
|---|---|---|---|---|---|---|---|---|---|---|
| experiment ID No. | [NaCl] (mol/L) | [NaBr] (mol/L) | [$NaNO_3$] (mol/L) | pH | $T$ (°C) | $NO_2$ | $Br_2$ | IBr | $I_2$ | BrCl |
| 1 | 1.0 | 0.05 | 1.0 | 2.5 | −25 | 378 | 17.9 | 3.8 | 0.44 | 0.06 |
| 2 | 1.0 | 0.05 | 1.0 | 2.5 | −25 | 414 | 15.8 | 3.8 | 0.22 | |
| 3 | 1.0 | 0.05 | 0.5 | 2.5 | −25 | 103 | 6.2 | 1.4 | | |
| 4 | 1.0 | 0.05 | 0.5 | 2.5 | −25 | 78 | 11.8 | 0.7 | | |
| 5 | 1.0 | 0.05 | 0.5 | 2.5 | −25 | 342 | 29.5 | 2.9 | 0.19 | |
| 6 | 1.0 | 0.05 | 0.1 | 2.5 | −25 | 149 | 12.1 | | | |
| 7 | 1.0 | 0.05 | 0.1 | 2.5 | −25 | 196 | 17.6 | 0.8 | | |
| 8 | 1.0 | 0.05 | 0.01 | 2.5 | −25 | 10 | 5.7 | 0.1 | | |
| 9 | 1.0 | 0.05 | 0.01 | 2.5 | −25 | 11 | 3.8 | 0.1 | 0.06 | |
| 10 | 1.0 | 0.01 | 0.01 | 2.5 | −25 | 37 | 2.7 | | | |
| 11 | 1.0 | 0.0016 | 0.01 | 2.5 | −25 | 22 | 3.6 | 0.1 | | |
| 12 | 1.0 | 0.0016 | 0.01 | 2.5 | −25 | 11 | 2.5 | 0.1 | | |
| 13 | 1.0 | 0.05 | 0.1 | 2.5 | −10 | 869 | 70.3 | 11.1 | 0.06 | 0.07 |
| 14 | 1.0 | 0.05 | 0.1 | 2.5 | −10 | 358 | 75.1 | 7.8 | 0.14 | |
| 15 | 1.0 | 0.01 | 0.1 | 2.5 | −10 | 537 | 26.2 | 2.9 | 0.08 | |
| 16 | 1.0 | 0.01 | 0.1 | 2.5 | −10 | 654 | 24.0 | 3.5 | | |

produced about 4 times more $NO_2$ than solutions frozen at 248 K. Bromine production increased by about a factor of 5 over the same temperature range. For example, for 1 M NaCl, 0.05 M NaBr, 0.1 M $NaNO_3$, pH 2.5, the average $Br_2$ fluxes were $1.5 \times 10^{12}$ molecules/cm$^2$/s at 248 K and $7.3 \times 10^{12}$ molecules/cm$^2$/s at 263 K. IBr production also exhibited a strong temperature dependence, but the signals were sufficiently close to detection limit to inhibit defining the increase accurately.

Although higher temperatures may increase rate constants between OH and a dissolved halide, the oxidation reactions are already fast, and the change in the kinetics due to the small temperature differences are likely to be small. Instead, other factors probably control why higher temperatures may increase the flux of $NO_x$ and halogens from the ice. Most importantly, the quantum yield of OH from nitrate photolysis decreases with temperature. Chu and Anastasio measured that the quantum yield for OH production in ice decreases by a factor of 3 with a 29 K decrease in temperature.[7] This decrease is similar to the change in fluxes that we observe over a 15 K temperature change.

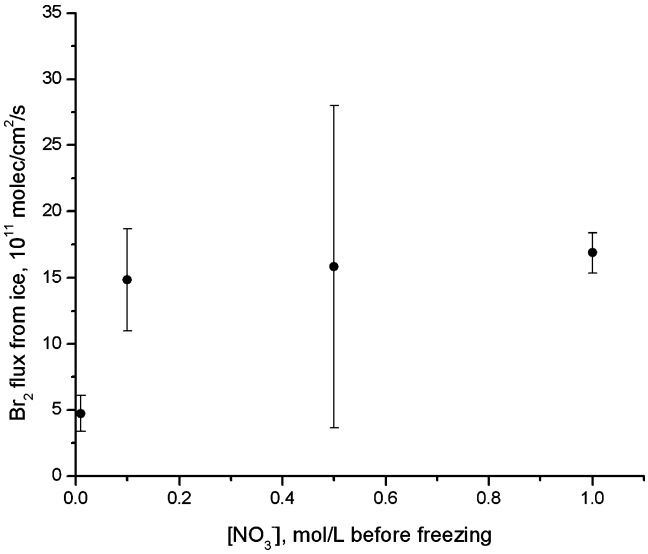


**Figure 5.** At 248 K, increased $Br_2$ production is observed as concentration of nitrate in the ice increases. 1.0 M NaCl, 0.05 M NaBr, pH = 2.5. The uncertainties in this plot and later plots are standard deviations used to indicate the variance within the data set; with only 2−3 points, they do not have statistical validity.

Also, the nature of the frozen solution is changing in character as temperature is lowered. Koop et al. showed that at 250 K, some sodium chloride crystallizes out of seawater solutions as $NaCl \cdot 2H_2O$.[26] The eutectic point of sodium nitrate is 255 K, and it stands to reason that a portion of nitrate would have crystallized out of solution between 263 and 248 K as well. This salt crystallization occurs concurrently with the formation of ice. Overall, the ionic strength of the liquid component of the frozen solution will increase as water crystallizes into a solid. George and Anastasio found that bromine release decreased with increases in the ionic strength of the liquid from which it evolved.[16] Thus, if these reactions are taking place in highly concentrated liquid pockets within the ice, as is likely, it follows that $Br_2$ production will be affected.

**3.5. Effect of Acidity on $Br_2$ Production.** Both halogen and $NO_x$ production decreased with decreasing acidity so that, at 248 K, the halogen fluxes from frozen pH 7 substrates did not give signals above detection limits. Instead, we report the acidity dependence at 263 K where, in early experiments, pH 7 solutions produced clearly measurable quantities of halogens. Although the CIMS was not calibrated absolutely at this time, in a relative sense these experiments showed that the $Br_2$ yields were between 1 and 2 orders of magnitude smaller when pH was raised from

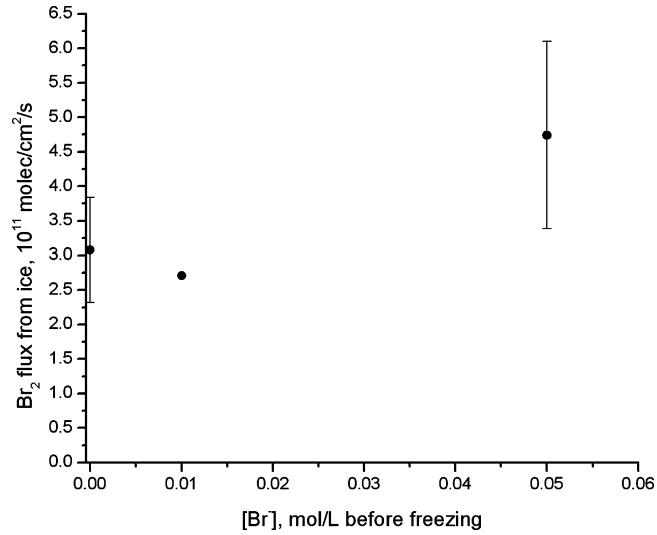


**Figure 6.** At 248 K, $Br_2$ production does not vary with concentration of bromide in the ice. 1.0 M NaCl; 0.01 M $NaNO_3$; pH = 2.5.

2 to 7 for solutions of 1.0 M NaCl, 0.05 M NaBr composition, with 0.1−1.0 M $NaNO_3$.

We note that both Frinak and Abbatt,[14] using a gas-phase source of OH, and George and Anastasio,[16] using a photolytic source, also observed greater $Br_2$ production from acidic solutions. This acidity dependence is consistent with known aqueous chemistry, as described in more detail by Frinak and Abbatt and by George and Anastasio.[14,16] Briefly, it is known that the reaction between dissolved OH and $Br^-$ ($k^{II} = 1.1 \times 10^{10}$ $M^{-1}$ $s^{-1}$)[12] is faster than the reaction between OH and $Cl^-$ ($k^{II} = 4.3 \times 10^9$ $M^{-1}$ $s^{-1}$).[27] However, since chloride ions outnumber bromide ions by a large ratio, the reaction of OH with chloride should dominate:

$$OH + Cl^- \leftrightarrow HOCl^- \quad (3)$$

$$HOCl^- + H^+ \rightarrow H_2O + Cl \quad (4)$$

$$HOCl^- + Cl^- \rightarrow Cl_2^- + OH^- \quad (5)$$

$$Cl^- + Cl \rightarrow Cl_2^- \quad (6)$$

$$Cl_2^- + Br^- \rightarrow BrCl^- + Cl^- \quad (7)$$

$$BrCl^- + Br^- \rightarrow Cl^- + Br_2^- \quad (8)$$

$$Br_2^- + Br_2^- \leftrightarrow Br_3^- + Br^- \quad (9)$$

$$Br_3^- \leftrightarrow Br_2 + Br^- \quad (10)$$

Note that the competition between 4 and 5 gives rise to the acidity dependence, with reaction 5 being quite slow. The net reaction becomes:

$$2OH^- + 2Br^- + 2H^+ \rightarrow Br_2 + 2H_2O \quad (11)$$

Note that the weak acidity dependence in the quantum yield for OH production, where OH yields actually increase slightly in going from pH 2 to pH 7,[7] is thought to be dominated by the chemistry just described.

It is also theoretically possible for $Cl_2^-$ to self-react and form molecular chlorine:

$$Cl_2^- + Cl_2^- \rightarrow Cl_2 + 2Cl^- \quad (12)$$

However, chlorine production is not observed in cases where sufficient quantities of bromide are available. For example, Frinak and Abbatt did not observe $Cl_2$ production from exposure of gas-phase OH with solutions where chloride ions outnumbered bromide ions by $3 \times 10^5$ to 1.[14] Similarly, we see no evidence for $Cl_2$ formation in our experiments.

Finally, we note that if some component of the halogen formation proceeds via HONO formation, then enhanced formation at low acidity would be consistent with HONO ($pK_a = 3.3$) being preferentially formed in Reaction 2.

**3.6. Gas-Phase $Br_2$ Yields Relative to OH Production.** We were interested to quantify the amount of OH that was forming in our experiments, so that we could relate it to the amount of $Br_2$ observed. Total OH production can be measured by adding an in situ OH scavenger, such as benzoic acid, to solutions[28] or ices[7] that do not contain other OH scavengers, such as bromide. Benzoic acid is susceptible to reaction with hydroxyl radicals, forming *p*-hydroxybenzoic acid among other products. After exposing an ice containing nitrate and benzoic acid to light, we used high performance liquid chromatography (HPLC) to quantify the amount of *p*-hydroxybenzoic acid formed.

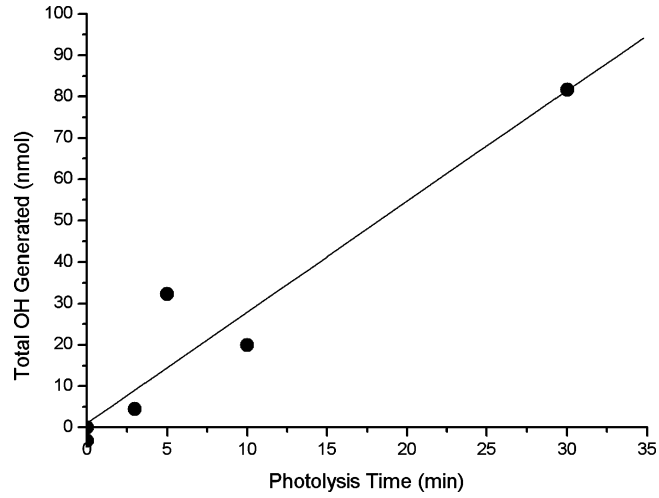


**Figure 7.** Total OH radical generation from photolysis as a function of time. These values come from the measured concentration of p-hydroxy benzoic acid produced in 7 mL solutions, and adjusted for the yield of this product in OH reaction.[7] Solutions contained 1.0 M NaCl, 0.1 M $NaNO_3$, 0.01 M sodium benzoate, pH = 2.5, 263 K.

Chu and Anastasio have used this method to measure the quantum yields of OH from nitrate photolysis in ice at 263 K and found that the temperature dependence of the quantum yield in ice can be modeled by the same regression line as the values in aqueous solution.[7] This suggests that the photolysis is occurring in a liquid portion of the ice, rather than in the ice bulk itself.

In our case, we exposed solutions (1.0 M NaCl, 0.1 M $NaNO_3$, 10 mM sodium benzoate, pH = 2.5, 263 K) to light in the same manner as for the other experiments described in this paper. No bromide was added to these solutions, since it would compete with benzoic acid as an OH scavenger. We found that OH is produced linearly over time up to 30 min (Figure 7), at a rate of 2.7 nmol/min = $2.7 \times 10^{13}$ molecules/s. Chu and Anastasio also found this relationship to be linear. For a 2 $cm^2$ illuminated area, this represents an OH production rate of $1.35 \times 10^{13}$ molecules/$cm^2$/s. This is significantly less than our observed $NO_2$ production rates for this ice (4 to $9 \times 10^{13}$ molecules/$cm^2$/s) indicating that not all $O^-$ species generated in Reaction 1 form OH. However, this OH production rate is quite similar to our observed $Br_2$ production rates ($8 \times 10^{12}$ molecules/$cm^2$/s), with about 0.6 $Br_2$ molecules formed for each OH produced. The overall uncertainty in this ratio is quite high, on the order of a factor of 2 or so. Note that the stoichiometry for the overall reaction of OH with $Br^-$ is for two OH radicals to form one $Br_2$ molecule (Reaction 11). So, our results confirm that every OH radical generated is indeed involved in halogen activation.

## 4. Atmospheric Implications and Conclusions

Our overall conclusion is that frozen solutions containing both halides and nitrate produce gas-phase halogens when illuminated

in the ultraviolet. For solutions with chloride concentrations much higher than bromide that, in turn, was much more prevalent than iodide, we find that $Br_2$ is the dominant halogen formed, with smaller but significant yields of IBr. Although observed in some experiments, the yields of BrCl and $I_2$ were very small, and $Cl_2$ was never observed.

Given that frozen halide solutions are known to contain concentrated brines down to low temperatures,[26] we believe that the halide oxidation occurs in such solutions. It is also known that a small amount of solutes are soluble in ice[29] and so, while there is no need to invoke chemistry occurring in or on the ice surfaces, we can not rule it out either. However, the observations are all consistent with an aqueous phase mechanism. In particular, we believe that OH is formed initially by nitrate photolysis, given that we observe $NO_2$ produced simultaneously. The dependence of the halogen fluxes upon nitrate and the lack of halogen formation in the absence of nitrate are in agreement with nitrate being the OH precursor. Indeed, observations by Chu and Anastasio have suggested that the photolysis of nitrate is occurring in the liquid portion of ice matrices.[7] Other evidence in support of an OH-mediated reaction mechanism comes from our earlier studies, where we observed that OH can heterogeneously oxidize frozen and aqueous halide solutions, forming gas-phase molecular halogens.[14,17] Also, George and Anastasio have shown that OH formation drives gas-phase bromine release, by using both nitrate and $H_2O_2$ as photolytic OH precursors. Although we can not rule out HONO oxidation of halides playing a role, we believe that OH is more important given that the quantum yield for OH formation from nitrate photolysis is substantially higher than that for HONO generation.[6,7] In agreement with this is the stoichiometric agreement between the OH and $Br_2$ production rates, suggesting that, to within experimental uncertainties, we do not need to invoke a HONO pathway.

The OH radical goes on to preferentially oxidize bromide, even when it is present at close to seawater compositions. We find that every OH radical is involved in halide oxidation, through the radical trap experiments. The acidity dependence is in agreement with a mechanism whereby the OH radical first reacts with a chloride ion, then driving chemistry that ultimately leads to bromine formation (Reactions 3−10). We note that the persistent observation of IBr, and the observation of $I_2$ in some experiments, suggests that OH also has the ability to oxidize $I^-$ in frozen solutions. Much less IBr and $I_2$ were observed than $Br_2$, which is likely attributable to the high abundance of chloride and bromide relative to iodide, which is only present as an impurity. IBr formation has also been observed for the heterogeneous reaction of OH with frozen halide solutions and crystallized salts.[17] We note that this chemistry is to be expected, given that the rate constant for reaction between aqueous OH and $I^-$ is similar to that for OH and $Br^-$,[30] that is, oxidation of both species by OH is highly efficient.

The relevance of the chemistry described in this paper will be largely to sea ice to which nitrate has been deposited from the atmosphere, probably in the form of $HNO_3$.[31,32] Or, the same chemistry may occur in the snowpack to which marine aerosols and nitrate have been deposited. Whereas the hydrogen ion concentrations in these substrates will not be as high as those used in most of our studies, we do note that we observed $NO_x$ and halogen release from pH neutral solutions as well. The acidity of sea ice and snowpack surfaces is not well-known, especially with respect to the degree of acidification that arises from $HNO_3$ deposition or deposition of acidic sulfate particles. Likewise, the nitrate concentrations in the polar regions are orders of magnitude lower than those we used, that is, they are probably on the order of $\mu$M.[33,34] However, we believe the chemical mechanism should not be dependent on the nitrate concentration, given that it is acting only as the source of the OH radical. That being said, an important next step would be to examine whether real-world samples of ice or snow do yield gas-phase halogens upon ultraviolet illumination.

**Acknowledgment.** The authors acknowledge the financial support of NSERC and CFCAS. We thank Jamie Donaldson for helping with the initial optical setup and for lending the photolysis cell used in this work, and we thank Scott Mabury for loan of the Xe lamp.

## References and Notes

(1) Domine, F.; Shepson, P. B. *Science* **2002**, *297*, 1506.
(2) Grannas, A. M.; Shepson, P. B.; Guimbaud, C.; Sumner, A. L.; Albert, M.; Simpson, W.; Domine, F.; Boudries, H.; Bottenheim, J.; Beine, H. J.; Honrath, R.; Zhou, X. L. *Atmos. Environ.* **2002**, *36*, 2733.
(3) Honrath, R. E.; Lu, Y.; Peterson, M. C.; Dibb, J. E.; Arsenault, M. A.; Cullen, N. J.; Steffen, K. *Atmos. Environ.* **2002**, *36*, 2629.
(4) Beine, H.; Colussi, A. J.; Amoroso, A.; Esposito, G.; Montagnoli, M.; Hoffmann, M. R. *Env. Res. Lett.* **2008**, *3*, 045005.
(5) Zepp, R. G.; Hoigne, J.; Bader, H. *Environ. Sci. Technol.* **1987**, *21*, 443.
(6) Dubowski, Y.; Colussi, A. J.; Boxe, C.; Hoffmann, M. R. *J. Phys. Chem. A* **2002**, *106*, 6967.
(7) Chu, L.; Anastasio, C. *J. Phys. Chem. A* **2003**, *107*, 9594.
(8) Honrath, R. E.; Guo, S.; Peterson, M. C.; Dziobak, M. P.; Dibb, J. E.; Arsenault, M. A. *J. Geophys. Res., [Atmos.]* **2000**, *105*, 24183.
(9) Bartels-Rausch, T.; Donaldson, D. J. *Atmos. Chem. Phys. Discuss.* **2006**, *6*, 10713.
(10) Hellebust, S.; Roddis, T.; Sodeau, J. R. *J. Phys. Chem. A* **2007**, *111*, 1167.
(11) Matheson, M. S.; Mulac, W. A.; Weeks, J. L.; Rabani, J. *J. Phys. Chem.* **1966**, *70*, 2092.
(12) Zehavi, D.; Rabani, J. *J. Phys. Chem.* **1972**, *76*, 312.
(13) Zafiriou, O. C. *J. Geophys. Res.* **1974**, *79*, 4491.
(14) Frinak, E. K.; Abbatt, J. P. D. *J. Phys. Chem. A* **2006**, *110*, 10456.
(15) Oum, K. W.; Lakin, M. J.; DeHaan, D. O.; Brauers, T.; Finlayson-Pitts, B. J. *Science* **1998**, *279*, 74.
(16) George, I. J.; Anastasio, C. *Atmos. Environ.* **2007**, *41*, 543.
(17) Sjostedt, S. J.; Abbatt, J. P. D. *Env. Res. Lett.* **2008**, *3*, 045007.
(18) Seisel, S.; Rossi, M. J. *Ber. Der Bunsen-Gesellschaft* **1997**, *101*, 943.
(19) Diao, G. W.; Chu, L. T. *J. of Phys. Chem. A* **2005**, *109*, 1364.
(20) Barrie, L. A.; Bottenheim, J. W.; Schnell, R. C.; Crutzen, P. J.; Rasmussen, R. A. *Nature* **1988**, *334*, 138.
(21) Schroeder, W. H.; Anlauf, K. G.; Barrie, L. A.; Lu, J. Y.; Steffen, A.; Schneeberger, D. R.; Berg, T. *Nature* **1998**, *394*, 331.
(22) Vogt, R.; Crutzen, P. J.; Sander, R. *Nature* **1996**, *383*, 327.
(23) Huey, L. G.; Hanson, D. R.; Howard, C. J. *J. Phys. Chem.* **1995**, *99*, 5001.
(24) Thornton, J. A.; Braban, C. F.; Abbatt, J. P. D. *Phys. Chem. Chem. Phys.* **2003**, *5*, 4593.
(25) *NIST Chemistry WebBook, NIST Standard Reference Database* No. 69; Linstrom, P. J.; Mallard, W. G., Eds.; 2010.
(26) Koop, T.; Kapilashrami, A.; Molina, L. T.; Molina, M. J. *J. Geophys. Res.* **2000**, *105*, 26393.
(27) Jayson, G. G.; Parsons, B. J.; Swallow, A. J. *J. Chem. Soc. - Faraday Trans. I* **1973**, 1597.
(28) Zhou, X. L.; Mopper, K. *Marine Chem.* **1990**, *30*, 71.
(29) Hobbs, P. V. *Ice Physics*; Clarendon Press: Oxford, 1974.
(30) Buxton, G. V.; Greenstock, C. L.; Helman, W. P.; Ross, A. B. *J. Phys. Chem. Ref. Data* **1988**, *17*, 513.
(31) Neubauer, J.; Heumann, K. G. *Atmos. Environ.* **1988**, *22*, 537.
(32) Jaffe, D. A.; Zukowski, M. D. *Atmos. Environ.* **1993**, *27*, 2935.
(33) Beine, H. J.; Domine, F.; Ianniello, A.; Nardino, M.; Allegrini, I.; Teinila, K.; Hillamo, R. *Atmos. Chem. Phys.* **2003**, *3*, 335.
(34) France, J. L.; King, M. D.; Lee-Taylor, J. *Atmos. Environ.* **2007**, *41*, 5502.

JP102072T